Progress In Electromagnetics Research C, Vol. 117, 41–54, 2021

Accurate Fault Location for Long-Distance Electric Transmission Lines

Lihui Zhao[1], Jingwei Zhu[1, *], Hongzhe Yang[2], and Tianhuai Qiao[1]

Abstract—This paper, using the distributed parameter line model, presents an accurate fault location method based on fundamental frequency positive sequence fault components for EHV transmission line. The method is based on positive sequence fault components Extra-High Voltage (EHV) electric transmission line. The method based on the positive sequence fault component is robust to the operating state of the prefault system and fault path resistance. The technique proposed in the paper does not require the fault type, fault phase, and the zero-sequence parameter to be obtained in advance. In addition, due to the use of fault component protection theory, the algorithm itself is not affected by the previous operating state of the system. The method uses a distributed parameter model, which is more accurate in positioning and smaller in error than a lumped parameter model by a large number of simulations. Accurate fault location is important for shortening the fault time and reducing the loss of the fault, so the positioning method proposed can improve the power supply quality and safety. This paper describes the characteristics of the proposed technique and assesses its performance by using Power Systems Computer Aided Design/Electromagnetic Transients including DC (PSCAD/EMTDC).

1. INTRODUCTION

Long-distance electric transmission lines are responsible for the transmission of electric energy and play an important role in the power system. Once the electric transmission line fails, the power transmission will be interrupted, which may cause major impacts until the fault is located and repaired [1, 2]. Fault location plays an important role in electric transmission line protection. Fast and accurate fault location helps to restore the power supply and stable operation of the power system as soon as possible.

The research on fault location methods began in the 1980s [3]. After continuous research by scholars, many fault location methods have been proposed. The fault location of electric transmission lines can be divided into three categories: fault analysis algorithm [4–6], traveling wave location algorithm, and intelligent location algorithm according to different location principles [7–9].

The fault analysis method uses relevant system parameters and the measured voltage and current to locate fault when the electric transmission line fails. For example, Using the measured voltage and current to calculate the impedance of fault circuit, technical staff can find the fault location according to the characteristics of the voltage distribution. There are two methods of obtaining electricity data: single-ended data method and double-ended data method [10].

The single-ended fault location algorithm uses only the voltage and current measured at the single end and necessary system parameters to calculate the fault distance. Since single-ended information is used only, which is simple and convenient to implement, the single-ended fault-location method has been widely used [11]. However, using only single-ended information cannot eliminate the effect of operation mode of the opposite system and, of the transition resistance, resulting in a large number of errors in

Received 29 September 2021, Accepted 2 December 2021, Scheduled 17 December 2021
* Corresponding author: Jingwei Zhu (zjwdl@dlmu.edu.cn).
[1] College of Marine Electrical Engineering, Dalian Maritime University, Dalian 116026, China. [2] School of Electrical Engineering, Shanghai Institute of Technology, Shanghai, China.

fault location results. In order to overcome adverse effects, continuous research has been focused on eliminating the effect of system operation mode and transition resistance.

The double-ended method uses the electrical quantity at both ends of the line. Due to the use of current and voltage at both ends, in principle, the method is not affected by transition resistance and system impedance on both ends [12, 13]. According to different electrical quantities required, the double-ended method can be subdivided into two-terminal current plus one-terminal voltage method and two-terminal voltage and current method. The former usually uses microwave channel or fiber channel, and distance measurement can be obtained with the received current data of the opposite terminal. The latter must use the communication channel to transmit the voltage and current data at two terminals. However, with the improvement of the automation level of power grid, it is very easy to exchange data between the two terminals of the line and the central dispatcher, and it can be widely promoted and applied.

The traveling wave method uses the time difference of traveling wave propagation between the fault point and the measurement point to measure the distance to the fault. In principle, the traveling wave method is not affected by factors such as the transition resistance at the fault point and the line structure. The traveling wave method has the advantages of high ranging accuracy and wide application range. The disadvantages lie in a problem with wave head recognition as well as required special equipment, large hardware investment, and complicated technology.

Beginning in the 1980s, intelligent positioning algorithm is the application of intelligent technology to power system fault analysis and location. The algorithm, which is used in fault location, combines traditional artificial intelligence technologies — machine learning algorithms including expert system (ES), backpropagation neural network (BPNN), Bayesian network (BN), support vector machine (SVM), etc. [14].

Machine learning is used in the processing of feature data, which is conducive to the fitting of nonlinear mapping relationships, and greatly improves the calculation performance and recognition accuracy. With the power system scale and nonlinear randomness increase, it is becoming more and more difficult to analyze the fault mechanism and characteristics based on the physical model. If the characteristics cannot well express the difference between the signals, the ranging results are not satisfactory [15].

Transmission line parameter models are divided into lumped parameters model and distributed parameters model [16]. The distributed parameter model considers the parameter distribution characteristics of the line, while the lumped parameter model does not consider them. The former is suitable in long-distance electric transmission lines, because long-distance lines cannot ignore the effects of line parameter distribution characteristics on the calculation results, and the latter is suitable in shorter long-distance lines. The authors have deduced in detail the fault location method based on the lumped parameter model in the published paper [17], and the length of the electric transmission line studied is 300 km. Later, when studying transmission lines with a length of more than 500 km, it is found that the positioning error of the proposed method becomes larger as the line length increases, and even reaches an unreceivable level.

Reference [17] realizes the fault location method of the transmission line under the lumped parameter model. The line model of this method is an approximate equivalent parameter model, and the distance measurement results under short transmission lines are relatively accurate. This paper is based on the distributed parameter model to achieve accurate fault location based on the characteristics of long-distance transmission lines. The core of the paper is in Section 2, giving the theory of the distributed parameter model and fault location derivation process. The advantage of the method lies in the accurate ranging results on long-distance transmission circuits. For some unexplained formulas in detail, please refer to [17].

The algorithm is the development of existing dual-terminal method. The algorithm uses sequence fault components. In principle, the positioning result is not affected by the fault type. The realization process of the algorithm includes an improved method of fault components extraction, differential filtering, and sequence component calculation. In the simulation, the different positioning results were compared, and the accuracy of the algorithm was proved.

2. PROPOSED FAULT-LOCATION FORMALIZATION

In this section, for long-distance electric transmission lines, a fault location method based on fundamental frequency positive sequence fault components is described with distributed parameter line model.

2.1. Basics of the Fault-Location Algorithm

A schematic diagram of a three-phase electric transmission line is shown in Fig. 1. Fig. 1 and Fig. 2 are taken from [17].

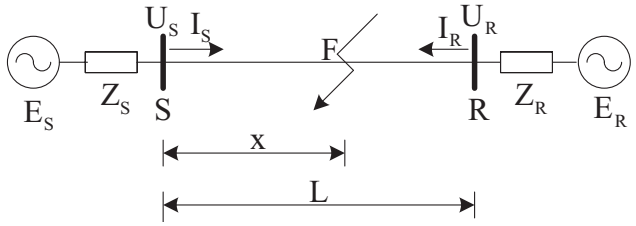

Figure 1. Transmission line for analysis.

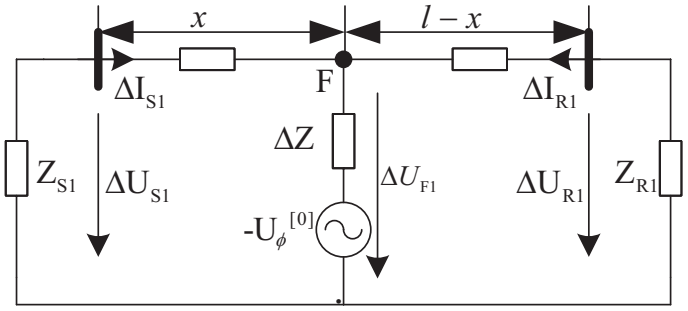

Figure 2. Positive sequence fault component diagram.

where,
F: fault location,
S: sending end of the line,
R: receiving end of the line,
l: transmission line length,
x: fault distance.
In Fig. 2, positive sequence fault component diagram is shown, where
Z_{s1}: transmitter positive sequence impedance,
Z_{R1}: receiver positive sequence impedance,
$\mathrm{U}_{\phi}^{[0]}$: special phase in case of asymmetric failure, arbitrary phase in case of symmetrical failure,
$-\mathrm{U}_{\phi}^{[0]}$: fictitious source voltage.

2.2. Fault Component Extraction Algorithm

This paper uses an improved fault component algorithm to extract the fault component. Compared with the usual method, the method in this paper has a better effect in the case of system oscillation and frequency deviation. The usual method uses Equation (1) to extract the fault component.

$$\Delta f(k) = f(k) - f(k - 2N) \tag{1}$$

where f is defined as electrical physical quantities such as voltage or current. N is the number of sampling points per cycle.

This paper adopts Equation (2) as the fault quantity extraction algorithm.

$$\Delta f(k) = [f(k) - f(k-2N)] - [f(k-2N) - f(k-4N)] \tag{2}$$

The advantages of Equation (2) to extract faults quantity are rigorously derived in the literature [17].

Comparing the results of Equations (1) and (2), using the fault component extraction method of Equation (2), the current is significantly smaller, which reduces the impacts of detection errors caused by system oscillations and frequency deviations.

2.3. Filtering, Amplitude and Phased Angle Compensation

Since the current after the fault component extraction contains DC and AC components, the paper uses Equation (3) to filter the DC component.

$$d\Delta i(t) = \Delta i(t) - \Delta i(t - \Delta T) \tag{3}$$

ΔT is the sampling period.

The amplitude and phase angle of the wave after the differential filter is different from that of the initial wave. Equation (4) is used to compensate the waveform. Equation (4) is valid when the sampling frequency is 2000 Hz. The numbers 6.37 and 85.8 are premised.

$$\Delta I_1 = \Delta \dot{I}_1' \cdot 6.37 \angle (-85.5^\circ) \tag{4}$$

ΔI_1 is the phasor current of initial fundamental frequency positive sequence.

2.4. Fault Location for Long Lines

Consider the distributed parameter model, the fault location algorithm is derived. Fig. 3 is a single-phase circuit diagram with uniformly distributed parameters, which describes the relationship between the voltage and current at the head of the line, and the voltage and current at the location of the line are x kilometers away from the head of the line, as shown in Equation (5).

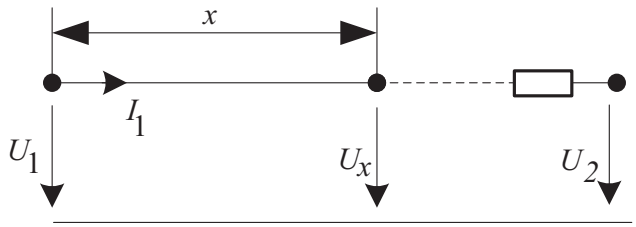

Figure 3. Distributed parameter circuit one-phase circuit diagram.

Considering the uniform distribution of lines in Fig. 3, Equation (5) can be obtained.

$$\left.\begin{aligned} U_1 &= U_x \cosh(\gamma x) + Z_c I_x \sinh(\gamma x) \\ I_1 &= \frac{U_x}{Z_c} \sinh(\gamma x) + I_x \cosh(\gamma x) \end{aligned}\right\} \tag{5}$$

where Z_c is the characteristic impedance, and γ is the transmission coefficient of the line. Strictly speaking, the wave impedance Z_c and the coefficient in Equation (5) are parameters in a single-phase circuit, but from the circuit principle, the positive, negative and zero sequence network of the three-phase circuit corresponding to the mathematical model established in the single-phase circuit can be clearly obtained. Therefore, Equation (5) is a formula for the positive sequence network in the three-phase circuit. Assuming $x = l$, the relationship between the voltage and current at both ends of the line is expressed as

$$\begin{bmatrix} U_1 \\ I_1 \end{bmatrix} = \begin{bmatrix} \cosh(\gamma l) & Z_c \sinh(\gamma l) \\ \dfrac{1}{Z_c} \sinh(\gamma l) & \cosh(\gamma l) \end{bmatrix} \begin{bmatrix} U_2 \\ I_2 \end{bmatrix} \tag{6}$$

From Equation (6), the line model can be regarded as a passive two-port network. The replaced equivalent circuit is shown in Fig. 4.

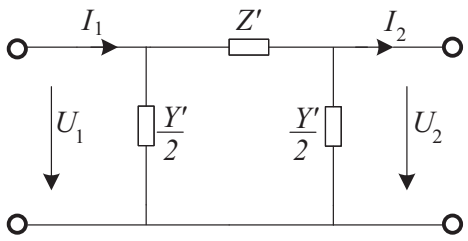

Figure 4. Line equivalent circuit.

From Fig. 4, the relationship equation between the voltage and current at both ends is as follows.

$$\left.\begin{aligned} U_1 &= \left(1+\frac{Z'Y'}{2}\right)U_2 + Z'I_2 \\ I_1 &= Y'\left(1+\frac{Z'Y'}{4}\right)U_2 + \left(1+\frac{Z'Y'}{2}\right)I_2 \end{aligned}\right\} \tag{7}$$

Comparing the coefficients of Equation (6) and Equation (7), we obtain

$$\left.\begin{aligned} 1+\frac{Z'Y'}{2} &= \cosh\gamma l \\ Z' &= Z_c\sinh\gamma l \\ Y'\left(1+\frac{Z'Y'}{4}\right) &= \frac{1}{Z_c}\sinh\gamma l \end{aligned}\right\} \tag{8}$$

From Equation (8), the precise line parameters are expressed as follows

$$\left.\begin{aligned} Z' = Z_c\sinh\gamma l &= Z\frac{\sinh\gamma l}{\gamma l} \\ Y' &= Y\frac{\tanh\frac{\gamma l}{2}}{\frac{\gamma l}{2}} \end{aligned}\right\} \tag{9}$$

$$\left.\begin{aligned} Z &= (r_1+jx_1)\,l = Z_1 l \\ Y &= (g_1+jb_1)\,l = Y_1 l \end{aligned}\right\}, \quad Z_c = \sqrt{\frac{Z_1}{Y_1}}(\Omega), \quad \gamma = \sqrt{Z_1Y_1}(1/\mathrm{km}) \tag{10}$$

Z', Y' are the precise series impedance and parallel admittance of the line, respectively. Z, Y are the total series impedance and parallel admittance after simply concentrating the distribution parameters of the line, respectively.

Figure 4 is a circuit diagram of a lumped parameter model, which is derived when a distributed parameter model is viewed as a two-port network. In Fig. 4, the relationship between the voltage and current at one end of the two-ports and that at the other end is shown in Equation (7). If Equation (7) and Equation (6) are completely equivalent, the lumped parameter circuit model in Fig. 4 can accurately describe a distributed parameter circuit model, which is derived from Equation (8). That is, Fig. 4 is a completely equivalent form to an accurate description of a distributed parameter model circuit with a lumped parameter circuit model that people are more accustomed to. Analyzing the impedance and admittance parameters marked in Fig. 4 and taking these parameters according to Equation (9), the lumped parameter circuit model of Fig. 4 can accurately describe as a distributed parameter circuit model.

For the electric transmission line not exceeding 300 km, the parameters of Equation (10) can be approximated. When the line is longer than 300 km, the line parameters of Equation (10) will lead to

larger calculation errors. The algorithm in this paper uses the exact parameters of Equation (9) to accurately calculate the distance to fault.

Considering the uniform distribution of lines in Fig. 3, Equation (5) can be rewritten as

$$\left.\begin{aligned} U_x &= U_1\cosh(\gamma x) - Z_c I_1 \sinh(\gamma x) \\ I_x &= -\frac{U_1}{Z_c}\sinh(\gamma x) + I_1\cosh(\gamma x) \end{aligned}\right\} \tag{11}$$

where

$$Z_c = \sqrt{\frac{Z_1}{Y_1}}, \quad \gamma = \sqrt{Z_1 Y_1}\,. \tag{12}$$

From Fig. 2, the voltage balance equation can be expressed as

$$\begin{cases} \Delta U_{F1} = \Delta U_{S1}\cosh(\gamma x) - Z_c \Delta I_{S1}\sinh(\gamma x) \\ \Delta U_{F1} = \Delta U_{R1}\cosh[\gamma(l-x)] - Z_c \Delta I_{R1}\sinh[\gamma(l-x)] \end{cases} \tag{13}$$

which can be rearranged as

$$e^{2\gamma x} = \frac{\Delta U_{R1}e^{\gamma l} - Z_c\Delta I_{R1}e^{\gamma l} - \Delta U_{S1} - Z_c\Delta I_{S1}}{\Delta U_{S1} - Z_c\Delta I_{S1} - \Delta U_{R1}e^{-\gamma l} - Z_c\Delta I_{R1}e^{-\gamma l}} \tag{14}$$

Defining

$$2\gamma = a1 + jb1 \tag{15}$$

$$\frac{\Delta U_{R1}e^{\gamma l} - Z_c\Delta I_{R1}e^{\gamma l} - \Delta U_{S1} - Z_c\Delta I_{S1}}{\Delta U_{S1} - Z_c\Delta I_{S1} - \Delta U_{R1}e^{-\gamma l} - Z_c\Delta I_{R1}e^{-\gamma l}} = a2 + jb2 \tag{16}$$

$a1$ and $b1$ are the real and imaginary parts of the propagation coefficient γ (the corresponding part is twice the part of Equation (12)). $\gamma = \sqrt{Z_1 Y_1}$, where $Z_1 = r_1 + jx_1\,(\Omega/\mathrm{km})$, Z_1 is the series impedance value per unit length of the line, and $Y_1 = g_1 + jb_1$ (s/km) is the parallel admittance value per unit length of the line). That is, $a1$ and $b1$ are known parameters when the line model specification has been determined.

The left side ΔU_{R1}, ΔI_{R1}, ΔU_{S1}, ΔI_{S1} of Equation (16) is the positive sequence fault component voltage and the positive sequence fault component current phasor that can be measured at both ends of the line. The left side Z_c and γ of the equation are the wave impedance and propagation coefficient, respectively, as shown in Equation (12). On the condition that models and specifications of the line have been determined, they are all known parameters, and the left side of the equation l is the full length of the line, which is also a known parameter.

According to Equations (15) and (16), we obtain

$$\begin{aligned} e^{2\gamma x} &= e^{x(a1+jb1)} = e^{xal}e^{jxb1} \\ &= e^{xa1}[\cos(xb1) + j\sin(xb1)] \\ &= a2 + jb2 \end{aligned} \tag{17}$$

Then

$$\begin{cases} e^{xa1}\cos(xb1) = a2 \\ e^{xal}\sin(xb1) = b2 \end{cases} \tag{18}$$

The distance between the measuring point and fault points is then solved as

$$x = \frac{\tan^{-1}\left(\dfrac{b2}{a2}\right)}{b1} \tag{19}$$

The above algorithm is applied to various types of faults on long-distance lines, which is proved by detailed numerical simulation.

3. EVALUATION OF THE FAULT LOCATION ALGORITHM

In order to evaluate the fault location algorithm proposed in this paper, the PSCAD/EMTDC software package is used to build a line model for simulation testing. The simulation system is shown in Fig. 1. The length of the line is 1000 km. The parameters of the system are gathered in Table 1. The parameters of the line are gathered in Table 2.

Table 1. Systems parameters.

Parameters	Systems	
	S	R
$\dot{E}_M$ [kV]	500	500
Z_1 [Ω]	1.10+j42.38	1.06+j43.92
Z_0 [Ω]	j29.29	j38.47
Angle	0°	−30°

Table 2. Line parameters.

l	value
Z_1	(0.0311+j0.125) Ω/km
Z_0	(0.2750+j0.898) Ω/km
C_1	10.85 nF/km
C_0	7.762 nF/km

The simulation presents the test results of different fault types and different faults with path resistances. Fault types include three-phase short-circuit (TPH), double-phase short-circuit (DPH), double-phase ground short-circuit (DPG), and single-phase ground short-circuit (SPG). The different states and initial conditions of the system, such as the starting angle of the fault, the transposition of the line, the load condition of the line, and the line parameters, may have an impact on the robustness of the algorithm, which is considered in the simulation of the algorithm.

3.1. Performance of the Fault Location Test

In this section, a large number of tests are completed. In order to verify the accuracy of the distributed parameter model on long-distance lines, the simulation gives the test results of the algorithm based on distributed parameters and lumped parameters.

The initial condition of the test system is described below. The phase angle difference of the systems at both ends is 30 degrees, the fault start angle is 0 degrees, and the start time of the fault time window is 0.2 s. For asymmetric faults (SPG, DPG, DPH) and symmetric faults (TPH), the fault initiation time was $t = 0.2$ s. All phasors were ideally synchronized. The system sampling frequency is 2 kHz, and the observation time window is 60 ms.

The simulations of metallic fault are shown in Fig. 5 to Fig. 6. FL1 in the simulation diagram is the fault location distance result based on the distributed parameter model. FL2 in the simulation diagram is the fault location distance result based on the lumped parameter model. The two fault location results are the location results of the same fault (the fault type and fault location are the same). The current and the location distance at the time of fault are presented by the method proposed in this paper. It can be seen from Fig. 5 to Fig. 6 that the algorithm for long-distance electric transmission lines is suitable for metallic faults. Positioning result can be accurately achieved after 20 ms.

Figure 7 shows the partially enlarged views of metallic fault simulations when fault point is set at 200 km from the measuring end. Regardless of symmetrical faults and asymmetrical faults, the

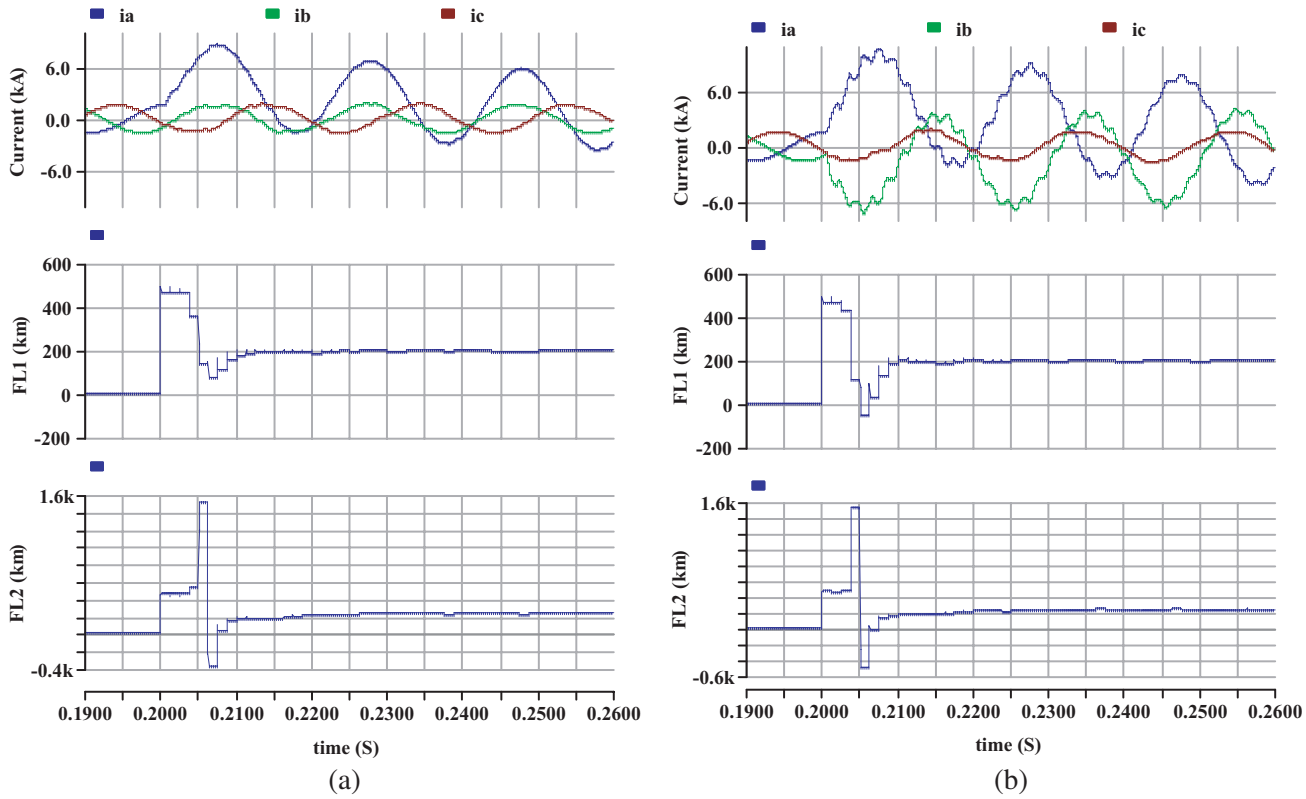

Figure 5. SPG and DPG of metallic faults. (a) SPG. (b) DPG.

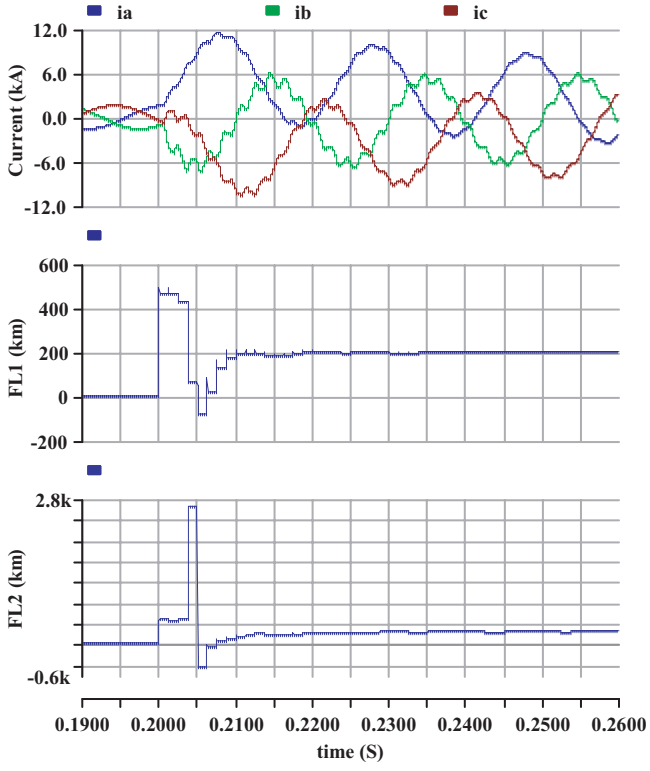

Figure 6. TPH of metallic faults.

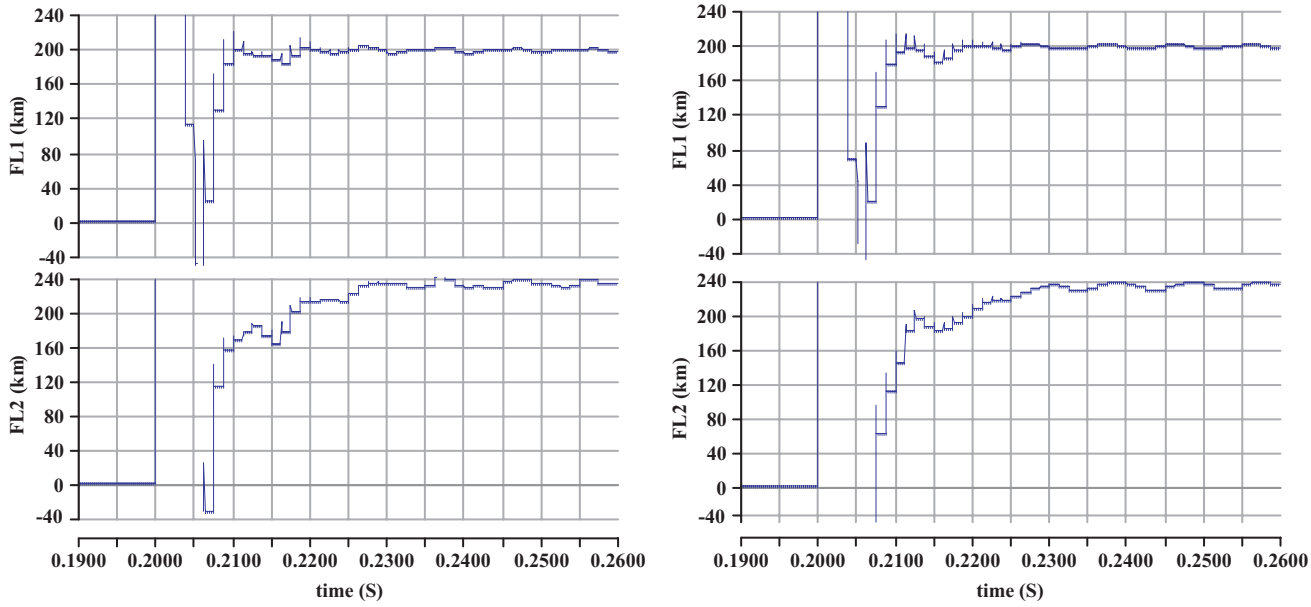

Figure 7. The partially enlarged view of SPG and TPH metallic fault.

positioning results based on the distributed parameter model are significantly more precise than the lumped parameters.

The simulations of metallic fault with path resistance are shown in Fig. 8 and Fig. 9. The SPG fault with a path resistance of 200 Ω and the phase-to-phase fault with a path resistance of 50 Ω (DPG, DPH and TPH) are evaluated. It can be seen from Fig. 8 to Fig. 9 that the algorithm for long-distance electric transmission lines is suitable for fault with path resistance. Similarly, the fault location method based on the distributed parameter model is more precise than the lumped parameters.

Figures 10 to 11 show the partially enlarged views of the simulations with fault resistance. After partial amplification processing, the differences of the fault location algorithm based on distributed parameters and lumped parameters are more obvious. Regardless of symmetrical faults and asymmetrical faults, the fault location method based on the distributed parameter model is more precise than the lumped parameters. For long-distance line, the advantages of the method proposed are more obvious.

3.2. Effect of Load Current

In order to measure the accuracy of positioning, the percentage error is defined as

$$\text{Error}\,(\%) = \frac{|l_{\text{exact}} - l_{\text{calc}}|}{l_{\text{exact}}} \cdot 100\% \tag{20}$$

where l_{exact} is the true fault distance, and l_{calc} is the distance to fault obtained by calculation.

Different types of faults under heavy load and light load were tested. Table 3 shows the test results. By comparing the positioning results under heavy load and light load, the proposed fault location method is not affected by load changes. The location result only depends on the actual fault location.

3.3. Effect of Untransposition

Many fault location methods assume that the line is completely transposed. In this paper, a non-full transposition model is established in PSCAD. The proposed fault location method is tested.

The results are shown in Table 4. The results show that the proposed fault location method is suitable for non-full transposition transmission lines.

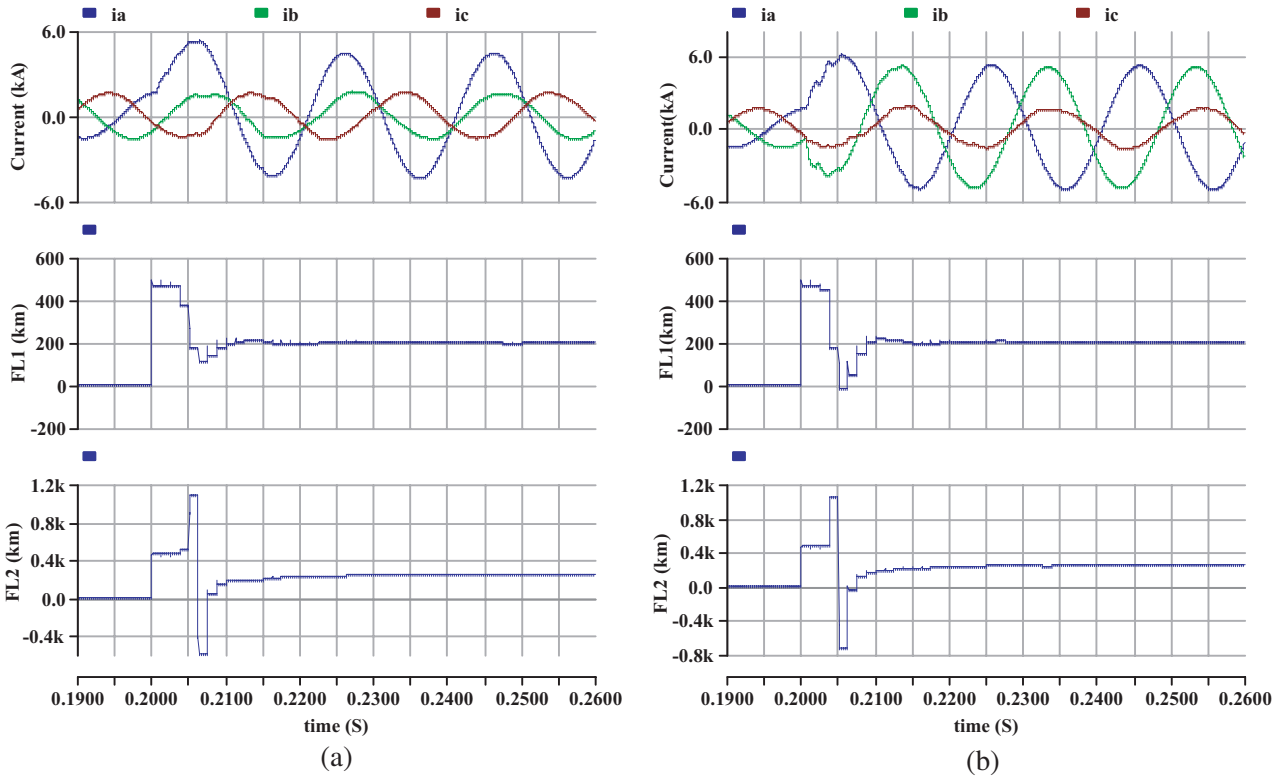

Figure 8. Simulation results of metallic fault with path resistance. (a) SPG with path resistance 200 Ω. (b) DPG with path resistance 50 Ω.

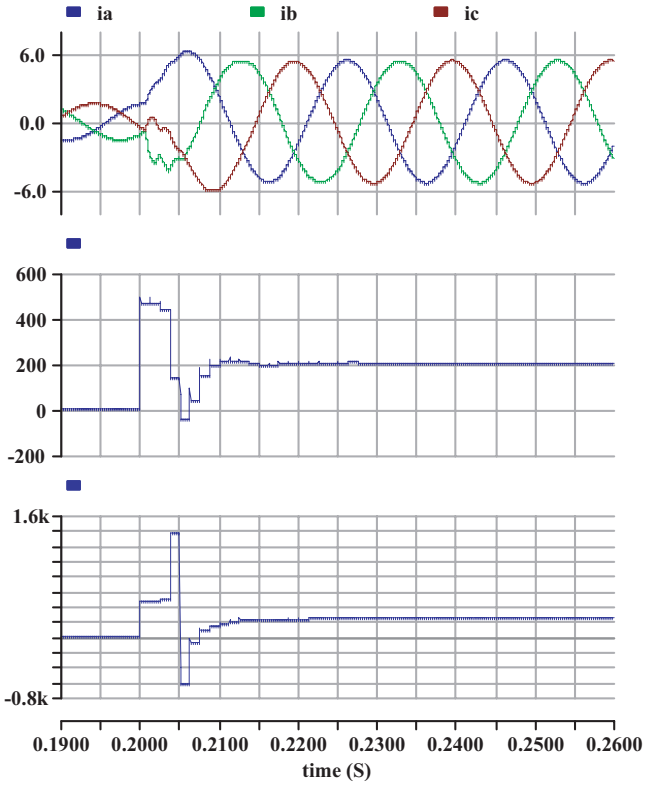

Figure 9. TPH with path resistance 50 Ω.

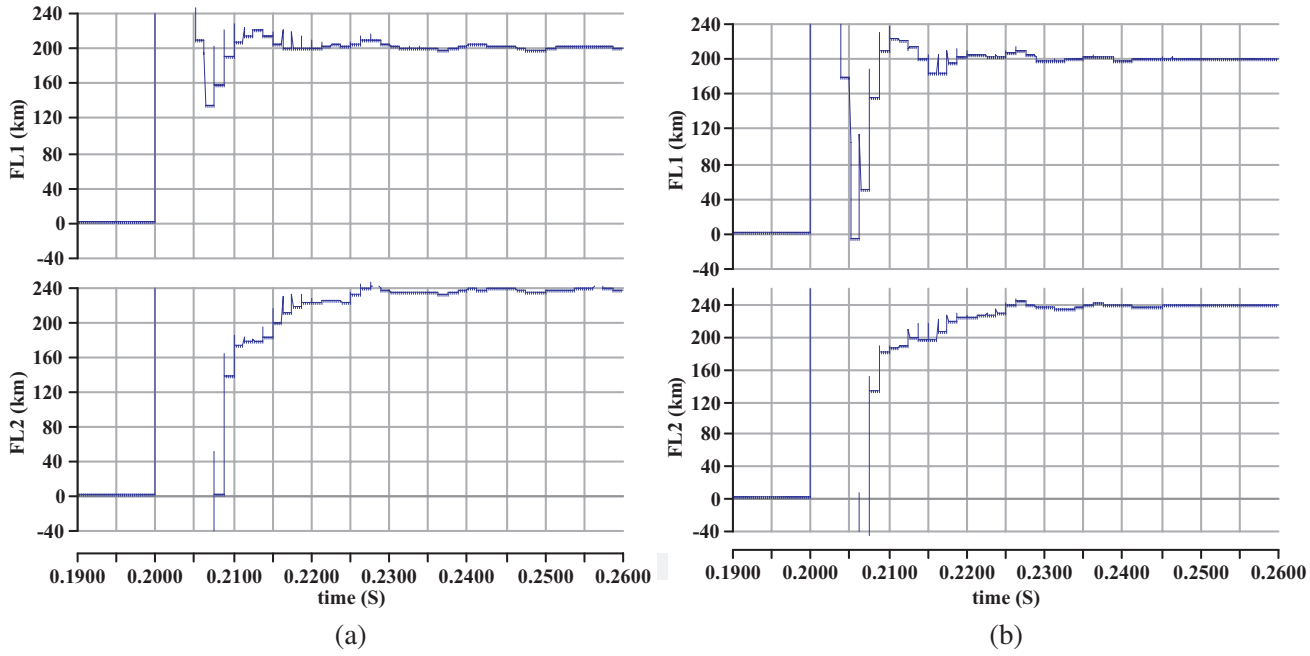

Figure 10. The partially enlarged view of the simulation results with fault resistance. (a) SPG with the resistance 200 Ω. (b) DPH with the resistance 50 Ω.

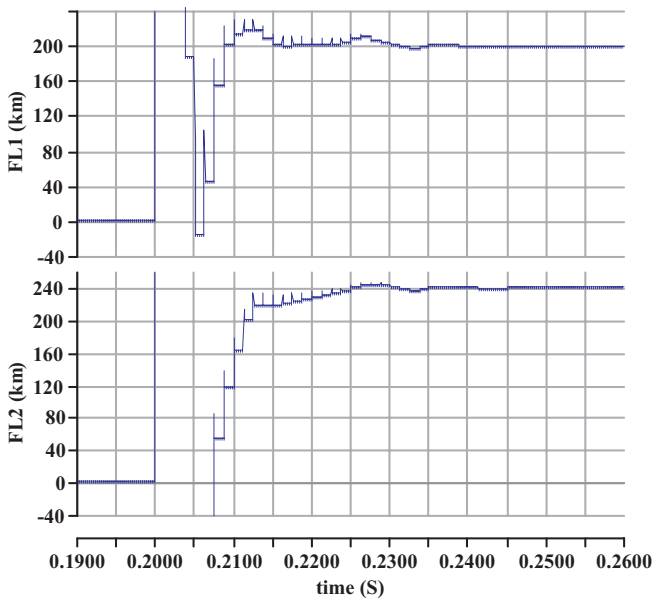

Figure 11. The partially enlarged view of TPH with the resistance 50 Ω.

3.4. Effect of Fault Inception Angle

The effect of fault inception angle on the accuracy of the algorithm for SPG, DPG and DPH is shown in Table 5. The fault inception angle varied from 0° to 180°. The results show that the proposed algorithm is independent of the fault inception angle with an average of 1.656, 1.575, 1.515 for SPG, DPG, and DPH, respectively.

Table 3. Effect of load current when SPG and TPH.

Load condition	Fault (km)	Estmi. FL (km)		Error of Estim. FL(%)	
		SPG	TPH	SPG	TPH
Light-load	120	122.16	123.16	1.800	2.633
	240	242.15	246.17	0.895	2.570
	360	361.65	365.31	0.458	1.302
	480	482.13	487.63	0.443	1.590
Heavy-load	120	122.56	124.1	2.133	3.410
	240	241.96	243.15	0.816	1.315
	360	356.5	365.14	0.972	1.427
	480	476.45	487.11	0.740	1.481

Table 4. Effect of untransposition when DPH and TPH.

Line condition	Fault (km)	Estmi. FL (km)		Error of Estim. FL(%)	
		DPH	TPH	DPH	TPH
transposed	80	84.39	83.02	5.487	3.775
	180	182.32	182.42	1.288	1.344
	280	276.14	284.63	1.378	1.653
	380	385.46	384.69	1.436	1.234
untransposed	80	86.39	86.39	0.639	4.287
	180	183.44	183.44	7.987	2.594
	280	277.13	277.13	1.025	2.271
	380	386.41	386.41	1.686	1.607

3.5. Effect of Line Parameters

The parameters of the real line are not easy to obtain accurately, and the positioning algorithm depends on the line parameters. At the same time, the line parameters are affected by the natural environment such as temperature and humidity.

In order to evaluate the effects of the algorithm on the accuracy when the line parameters change, the experiment changes the line parameters within 10%. We divide the data into five groups for multiple tests. The test results obtained are shown in Table 6. The test shows that the measurement error varies within a certain range. In order to obtain more accurate line parameters, online measurement technology is needed.

From the above theoretical derivation and digital simulation, the fault location method based on distributed parameters proposed in this paper can be fully applied in engineering practice. The power required to be measured is the positive sequence fault component voltage and the positive sequence fault component current phasor on both sides of the line. In the era of microcomputer protection, only voltage and current transformers are required for the measurement of these power quantities, without any special equipment.

This paper mainly focuses on the theory and simulation of long-distance transmission lines. Due to the particularity of the Extra-High Voltage power system, there is no experimental verification under the current laboratory conditions. In the follow-up research, it is planned to take several dynamic simulations and field short-distance low-voltage lines for experimental research.

Table 5. Effect of fault inception angle.

Fault Type	Fault Inception angle (∘)	Estmi. FL (km)	Error of Estim. FL (%)
SPG	0	203.11	1.555
	45	203.56	1.780
	90	203.42	1.710
	180	203.16	1.580
DPG	0	202.95	1.475
	45	202.84	1.420
	90	203.68	1.840
	180	203.13	1.565
DPH	0	202.55	1.275
	45	202.61	1.305
	90	203.45	1.725
	180	203.51	1.755

Table 6. Results of line parameters.

group	Average error of estim	Max error (%)	min error (%)
1	0.561	1.621	0.311
2	0.862	2.650	0.593
3	0.752	0.953	0.460
4	1.361	2.256	0.875
5	1.051	1.893	0.631

4. CONCLUSIONS

This paper presents an accurate fault location algorithm for EHV long line based on fundamental frequency fault components. Using distributed parameters as the line model, a precise fault location technique is realized by synchronously collecting the voltage and current at both ends of the line.

The paper deduces the algorithm derivation process in detail. For different fault types, fault points, and line parameters, a lot of tests have been done through PSCAD. The results show that the algorithm is not affected by transition resistance, fault type, fault inception angle, load current, and line transposition. Comparing distributed parameters with lumped parameters, this algorithm has higher accuracy for long lines. When the line parameters change, the algorithm is also robust.

ACKNOWLEDGMENT

This work were supported by the National Natural Science Foundation of China under Project 51777024, 61806126.

REFERENCES

1. Phadke, A. G., M. Izumi, M. Yokoyama, K. Umemoto, T. Hlibka, and M. Ibrahim, "Fundamental basis for distance relaying with symmetrical components," *IEEE Trans. Power App. Syst.*, Vol. 96, No. 3, 635–646, 1977.

2. Kezunovic, M. and B. Perunicic, "Automated transmission line fault analysis using synchronized sampling at two end," *IEEE Trans. Power Del.*, Vol. 11, No. 1, 121–129, 1988.
3. Takagi, T., Y. Yamakoshi, J. Baba, K. Uemura, and T. Sakaguchi, "A new algorithm of an accurate fault location for EHV/UHV transmission lines: PART I — Fourier transformation method," *IEEE Trans. Power App. Syst.*, Vol. 3, No. 3, 1316–1323, 1981.
4. Lopes, F., K. M. Dantas, K. M. Silva, and F. B. Costa, "Accurate two-terminal transmission line fault location using traveling waves," *IEEE Trans. Power Del.*, Vol. 33, No. 2, 873–880, 2018.
5. Liao, Y. and S. Elangovan, "Improved symmetrical component-based fault distance estimation for digital distance protection," *IEE Proc. Gener. Transm. Distrib.*, Vol. 145, No. 6, 739–746, 1998.
6. Apostolopoulos, C. A. and G. N. Korres, "A novel algorithm for locating faults on transposed/untransposed transmission lines without utilizing line parameters," *IEEE Trans. Power Del.*, Vol. 6, No. 2, 2328–2338, 2010.
7. Kawady, T. and J. Stenzel, "A practical fault location approach for double circuit transmission lines using single end data," *IEEE Trans. Power Del.*, Vol. 18, No. 4, 1166–1173, 2003.
8. Livani, H. and C. Y. Evrenosoglu, "A machine learning and wavelet-based fault location method for hybrid transmission lines," *IEEE Trans. Smart Grid*, Vol. 5, No. 1, 51–58, 2014.
9. Terzija, V., Z. M. Radojevic, and G. Preston, "Flexible synchronized measurement technology-based fault locator," *IEEE Trans. Smart Grid*, Vol. 6, No. 2, 866–873, 2015.
10. Elsadd, M. A. and A. Y. Abdelaziz, "Unsynchronized fault-location technique for two- and three-terminal transmission lines," *Electric Power Systems Research*, Vol. 158, 228–239, 2018.
11. Elkalashy, N., T. A. Kawady, W. M. Khater, and A. M. I. Taalab, "Unsynchronized fault-location technique for double-circuit transmission systems independent of line parameters," *IEEE Trans. Power Del.*, Vol. 99, No. 4, 1591–1599, 2015.
12. Zhang, Y., J. Liang, Z. H. Yun, and X. M. Dong, "A new fault-location algorithm for series-compensated double-circuit transmission lines based on the distributed parameter model," *IEEE Trans. Power Del.*, Vol. 33, No. 6, 3249–3251, 2018.
13. Xu, Z., Z. Q. Du, L. Ran, Y. K. Wu, and Q. X. Yang, "A current differential relay for a 1000-kV UHV transmission line," *IEEE Trans. Power Del.*, Vol. 19, No. 4, 1392–1399, 2007.
14. Lin, Y., C. W. Liu, and C. S. Chen, "A new PMU-based fault detection/location technique for transmission lines with consideration of arcing fault discrimination — Part I: Theory and algorithms," *IEEE Trans. Smart Grid*, Vol. 19, No. 4, 1588–1593, 2004.
15. Lee, Y., C. H. Chao, T. C. Lin, and C. W. Liu, "A synchro phasor-based fault location method for three-terminal hybrid transmission lines with one off-service line branch," *IEEE Trans. Power Del.*, Vol. 33, No. 6, 3249–3251, 2018.
16. Terzija, V., Z. M. Radojevic, and G. Preston, "Flexible synchronized measurement technology-based fault locator," *IEEE Trans. Smart Grid*, Vol. 6, No. 2, 866–873, 2015.
17. Zhao, L., J. W. Zhu, and B. Gu, "A new technique based on fundamental frequency positive sequence fault components for fault location," *IEEJ Transactions on Electrical and Electronic Engineering*, Vol. 15, 536–543, 2020.